

BULLETIN OF THE CHEMICAL SOCIETY OF JAPAN, VOL. 46, 1346—1353 (1973)

## Chemical Approach to the Radiolysis of Polyphosphate Glass. I. Effects of Sb(III, V), Mo(V, VI) and U(IV, VI) Ions

Yoshimitsu KOBAYASHI and Niro MATSUURA

*Department of Pure and Applied Sciences, College of General Education,  
University of Tokyo, Komaba, Meguro-ku, Tokyo*

(Received September 16, 1972)

The yields of radiation-induced electrons and holes trapped in the glass matrix are easily determined by introducing metal ions, such as Sb, Mo, and U ions, into water-soluble  $\text{NaPO}_3$  polymer glass. Doping 1 mol % of these ions of a lower oxidation state wholly prevents the trapping of holes and results in oxidation to their higher oxidation states. A reaction in the reverse direction also occurs for the same ions of a higher oxidation state, which are converted into a lower one by reduction. This radiation-induced redox reaction has a minimum yield at a dopant composition corresponding to  $\text{Sb}_2\text{O}_4$  for Sb(III)–Sb(V),  $\text{Mo}_6\text{O}_{17}$  for Mo(V)–Mo(VI), and  $\text{U}_3\text{O}_8$  for U(IV)–U(VI) redox couples. The largest effective volume among these ions for capturing the holes is for Sb(III). In a high-dose region ( $10^{20}$  to  $10^{21}$  eV/g), the yields of the redox products of these ions increase logarithmically with the  $\gamma$ -dose absorbed. This makes it difficult to determine the G-value of the redox products precisely. The approximate values are in an order of magnitude of 0.1 atom per 100 eV absorbed.

The radiation-induced rupture of a chemical bond in a solid polyphosphate glass causes paramagnetic or

color centers. The results of a number of authors<sup>1–8)</sup> are in agreement with a model which assigns the radia-

1) A. Barkatt, M. Ottolengli, and J. Rabani, *J. Phys. Chem.*, **76**, 203 (1972).

2) A. Treinin; "Radical Ions" Ed. by E. T. Kaiser and L. Kevsn, Interscience Pub. N. Y. (1968), p. 525.

3) T. Feldman, A. Treinin, and V. Voltera; *J. Chem. Phys.*, **42**, 3366 (1965), *ibid.*, **47**, 2754 (1967).

4) Sakka, *Bull. Inst. Chem. Res. Kyoto Univ.*, **48**, 53 (1970).

5) J. C. Stroud, *J. Chem. Phys.*, **43**, 2442 (1965); *ibid.*, **37**, 836 (1962).

6) Y. Nakai, This Bulletin, **38**, 1308 (1965).

7) M. C. R. Symons, S. Subramanian, and H. W. Wardale, *J. Chem. Soc., A*, **1970**, 1239; *ibid.*, 1988 (1970).

8) M. Miura and A. Hasegawa, This Bulletin, **40**, 2553 (1967); *ibid.*, **39**, 1432 (1966).

tion-induced visible colors to holes (electron-deficient centers), each trapped in a network forming a P-O tetrahedron with one or more non-bridging oxygen atoms present in a polyphosphate chain.<sup>2)</sup> It is interesting to study from the chemical point of view the nature of these color centers by means of additives introduced into the glass as scavengers of the reactive species produced by radiation.<sup>3-6)</sup> A systematic survey was undertaken to find the most adequate additive for estimating the quantitative yields of primary species, holes and electrons. Sodium polyphosphate is a water-soluble glass which is suitable for chemical treatment after exposure to  $\gamma$ -rays.

The change in the optical absorption in irradiated glass was compared with the products in aqueous solution of irradiated glass. Among the dozen additives so far investigated, this paper will treat the redox couples, Mo(V)-Mo(VI), Sb(III)-Sb(V), and U(IV)-U(VI), preferably employed as additives because their visible absorption spectra are separated from the optical absorptions due to holes.

### Experimental

**Preparation of the Glass.** The base glass was prepared by the dehydration of  $\text{NaH}_2\text{PO}_4 \cdot 2\text{H}_2\text{O}$  to which appropriate amounts of metal oxide, less than 1 mol %, had been admixed. The fusion was carried out in a platinum crucible, principally at 800 °C for 3 hr in air, in order to prepare the Sb(III), Mo(VI), and U(VI) doped glasses. For preparing the U(VI) doped glass,  $\text{UO}_2(\text{CH}_3\text{CO}_2)_2 \cdot 2\text{H}_2\text{O}$  was employed in place of its oxide.<sup>9)</sup> The U(IV) and Mo(V) enriched glasses should be melted in the presence of reducing agents under a reducing atmosphere or under vacuum of  $10^{-6}$  Torr. The reducing atmosphere is effected by the use of a graphite crucible surrounded with a pile of graphite rods in an electric furnace or a quartz vessel placed in a vacuum line for vacuum melting.

**Optical Measurements.** The molten glass was poured into a brass mold with a rectangular form 8.3 mm thick, or it was chilled between two brass plates 2 mm apart. In order to eliminate the difference in the sample thickness and the scattering condition of the sample surface, a small correction was made by the normalization of background absorptions at about 700 nm. The spectra were taken and registered for optical absorption with an EPS-2 Model Hitachi Spectrophotometer, and for ESR spectra, with Japan Electron Optics Lab's JES-2BX model at a microwave frequency of 9400 Mc/s operating with 100 Kc/s field modulation. The molar extinction coefficient was determined by chemical analysis for Mo(V) as  $\epsilon = 17 \text{ M}^{-1} \text{ cm}^{-1}$  and for U(IV) as  $\epsilon = 32.1 \text{ M}^{-1} \text{ cm}^{-1}$ .

**Irradiation.** The sample was irradiated with a  $\text{Co}^{60}$   $\gamma$ -ray source of  $3.8 \times 10^{18} \text{ eV/g} \cdot \text{hr}$  10 cm from the center in the Institute for Solid State Physics, the University of Tokyo. For the highdose irradiation a  $\text{Co}^{60}$  source of  $1.8 \times 10^{19} \text{ eV/g} \cdot \text{hr}$  was occasionally used. The irradiations and measurements were performed at room temperature, and the  $\gamma$ -dose calibration was carried out with a Fricke dosimeter, assuming that  $G(\text{Fe}^{3+}) = 15.5^{10}$  and that the electron density per unit mass

was identical between the glass and Fricke's solution.

**Chemical Analysis.** The chemical analysis of antimony was made by colorimetry with Folin's reagent for Sb(III) and with Rhodamine B as the reagent for Sb(V).<sup>11)</sup> Antimony-doped samples were dissolved in dilute hydrochloric acid (2:1) to prevent the hydrolysis of  $\text{HSbCl}_6$  to an irreversibly-aquated form of  $\text{HSb}(\text{OH})_n\text{Cl}_{6-n}$ .<sup>12,13)</sup> Reproducible results were obtained when the dissolution of irradiated samples in hydrochloric acid was effected under the same conditions for a series of runs. The potentiometric titration of Mo(V) with 0.05N  $\text{K}_2\text{Cr}_2\text{O}_7$ <sup>14)</sup> was made after dissolving the irradiated glass in 2N HCl over a water bath for 0.5 hr in order to ensure the decomposition of the polymer phosphate into the monomer. For U(IV), irradiated samples were dissolved in a 5% sulfuric acid solution by bubbling nitrogen gas through the solution to prevent the oxidation of U(IV) to U(VI) due to air oxygen<sup>15)</sup> and by keeping the sample solution at about 80 °C during the dissolution in order to effect the complete hydrolysis of polyphosphate. The titration was effected by the addition of excess amounts of a  $\text{FeCl}_3$  solution by the use of diphenylamine as an indicator. For the titration of the total uranium content, a 5% sulfuric acid solution of the sample glass was passed through a Jones's reductor, after which the resultant U(IV) solution was titrated in the same way.<sup>16)</sup>

### Results and Discussion

**Sb Doped Glass, Effect of Antimony Ions.** Upon the  $\gamma$ -irradiation of the polyphosphate glass, an optical absorption due to trapped holes appears with a maxi-

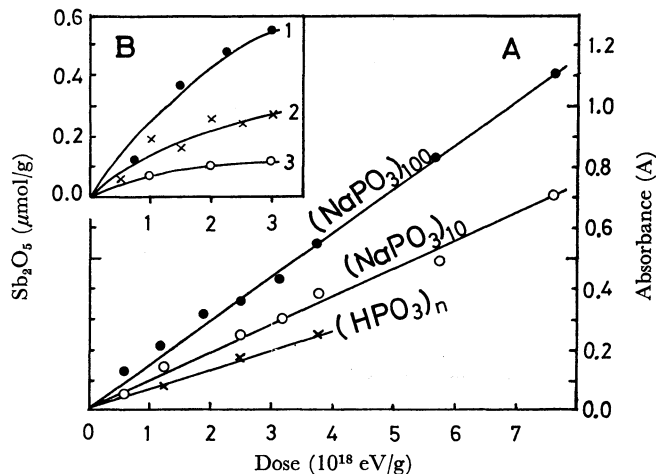


Fig. 1. A: Optical absorption at 510 nm of  $\gamma$ -irradiated polyphosphate glass with optical path 8.3 mm.

B: Yields of antimony (V) oxide, in  $\mu\text{mol/gram}$  of  $\text{NaPO}_3$ , from antimony (III) oxide doped glass under  $\gamma$ -ray irradiation. 1: 0.5 mol % of  $\text{Sb}_2\text{O}_3$  doped, 2: 0.25 mol% of  $\text{Sb}_2\text{O}_3$  doped and 3: 0.125 mol% of  $\text{Sb}_2\text{O}_3$  doped. Abscissa the same scale of unit with A.

- 11) N. Matsuura and M. Kojima, *Japan Analyst*, **6**, 155, 205 (1957).
- 12) H. M. Neumann, *J. Amer. Chem. Soc.*, **76**, 2611 (1954); C. H. Cheek and H. M. Neumann, *Anal. Chem.*, **27**, 1683 (1955).
- 13) N. A. Bonner, *J. Amer. Chem. Soc.*, **71**, 3909 (1949).
- 14) C. E. Cruthamel and C. E. Johnson, *Anal. Chem.*, **26**, 1284 (1954).
- 15) J. Halpern and J. G. Smith, *Can. J. Chem.*, **34**, 1419 (1956).
- 16) I. M. Kolthoff and J. J. Lingane, *J. Amer. Chem. Soc.*, **55**, 1871 (1933).

9) M. Mano and S. Ohashi, *This Bulletin*, **42**, 3616 (1969); *ibid.*, **43**, 84 (1970).

10) M. Haissinsky, "La Chimie Nucleaire et ses Applications," Masson, Paris (1957), p.333, N. Miller in "Actions Chimiques et Biologiques des Radiations," Vol. 2, Masson, Paris (1956), p.149.

mum peak at 510 nm. Figure 1A shows that the increase in absorbance is proportional to the  $\gamma$ -dose absorbed. The glasses with a mean chain length of phosphate smaller than that of Graham salt have smaller absorptions, and the polyphosphate glass of a chain less than 10 is no more transparent.<sup>17)</sup> For Graham salt, with an average chain length of 50 to 100, the optical absorption induced by irradiation is approximately the same, irrespective of the condition used in preparing the sample glass. When the exposure is prolonged beyond a certain limit,  $10^{19}$  eV/g, the change in absorption is no longer linear with the dose, but increases much more slowly.

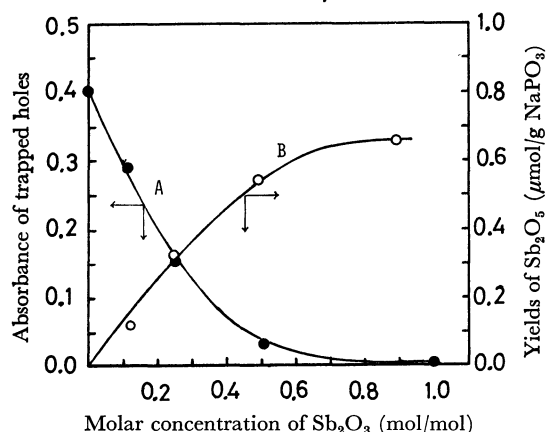


Fig. 2. A: Optical absorbancy at 510 nm due to trapped holes in  $\text{NaPO}_3$  glass as function of doped  $\text{Sb}_2\text{O}_3$  molar concentration ( $\text{Sb}_2\text{O}_3$  mol/ $\text{NaPO}_3$  mol)  
B: Yields of  $\text{Sb}_2\text{O}_5$  in  $\mu\text{mol/g NaPO}_3$  from  $\text{Sb}_2\text{O}_3$  doped in  $\text{NaPO}_3$  glass after  $\gamma$ -irradiation of  $3 \times 10^{19}$  eV/g with variation of doped  $\text{Sb}_2\text{O}_3$  concentration ( $\text{Sb}_2\text{O}_3$  mol/ $\text{NaPO}_3$  mol)

Antimony oxide, if one mole % is doped as  $\text{Sb}_2\text{O}_3$  into polyphosphate glass, entirely suppresses the appearance of the red color due to holes. Pentavalent antimony oxide,  $\text{Sb}_2\text{O}_5$ , is ineffective unless a greater part of the antimony(V) is converted into antimony(III) by thermal decomposition during the melting of a glass at a temperature higher than  $650^\circ\text{C}$ . The optical absorption at 510 nm decreases exponentially with respect to the concentration of Sb(III). The exponential curve shown in Fig. 2 makes it possible to calculate the effective capture volume of Sb(III) as a hole-formation inhibitor using Stroud's Eq. (1).<sup>5)</sup>

$$D_{h^+} = D_{h^+}^0 \cdot \exp(-v \cdot C) \quad (1)$$

In Eq. (1),  $D_{h^+}$  and  $D_{h^+}^0$  are the optical absorbances of the hole in the presence and in the absence of the Sb(III) inhibitor,  $C$ , the concentration of Sb(III), and  $v$ , the effective volume of the inhibitor against hole formation by radiation. The concentration of  $\text{Sb}_2\text{O}_3$ ,  $C$  for  $D_{h^+}/D_{h^+}^0 = 1/e$ , is found from Fig. 2 to be 0.125 mol % per one formula weight of  $\text{NaPO}_3$ . The effective capture volume,  $v$ , is calculated as  $3.8 \times 10^5 \text{ \AA}^3$ , which is a hundred times as large as the volume occupied by the  $\text{Sb}_2\text{O}_3$  molecule in the form of Valentinite.<sup>18)</sup>

17) N. Matsuura, T. K. Lin, and Y. Kobayashi, *This Bulletin*, **43**, 2850 (1970).

18) N. A. Antropov, V. P. Barzakovskii, I. A. Bondari, and U. P. Udalov; "Phase Diagrams of Silicate System" A. N. (1970), p. 203.

**Redox Yields of Sb in Glass.** The initial  $G$ -values determined for  $3 \times 10^{18}$  eV/g or less are surprisingly large both with respect to the oxidation of Sb(III) to Sb(V) for  $\text{Sb}_2\text{O}_3$  doped glass and with respect to the reduction of Sb(V) to Sb(III) for  $\text{Sb}_2\text{O}_5$  doped glass. The curves represented in Figs. 1B and 2B demonstrate an extraordinary high yield of Sb(V), which attains, in the  $G$ -value, some ten molecules of  $\text{Sb}_2\text{O}_5$  per 100 eV of  $\gamma$ -energy absorption. Such a  $G$ -value can not be expected from the mechanism of a radiation-induced redox reaction in a solid currently accepted in radiation chemistry.<sup>19)</sup> However, in a higher dose region the  $G$ -values of Sb(V) formation in Sb(III) doped glass are greatly reduced to an ordinary value of around 0.1. The yields of Sb(III) from Sb(V) in irradiated glass are much more pronounced, attaining a  $G$ -value of several hundred in the low-dose region. The Sb(V) content of 1 mol%  $\text{Sb}_2\text{O}_5$  doped glass prepared at  $650^\circ\text{C}$  for 3 hr showed  $90 \mu\text{mol}$  of  $\text{Sb}_2\text{O}_5$  per gram of  $\text{NaPO}_3$  glass before irradiation. This was decreased to  $70 \mu\text{mol/g}$  after irradiation at a dose of  $3 \times 10^{18}$  eV/g. The data obtained are very few and not reliable enough for us to predict the mechanism of the radiation-induced reduction of Sb(V) to Sb(III), because the background content of Sb(III), increased upon thermal treatment before irradiation, surpasses the amount produced by radiation.

Since several oxides, such as  $\text{Sb}_6\text{O}_{13}$  and  $\text{Sb}_2\text{O}_4$ , are known<sup>20)</sup> as stable phases in a pure antimony oxide system at a temperature between  $650$  and  $900^\circ\text{C}$ , these species must be considered in addition to Sb(III) and Sb(V) oxides as major components in a molten glass. Accordingly, the chemical analysis of Sb(III) and Sb(V) was undertaken to see if there was a difference in the average oxidation state of antimony between pure oxide and the same oxide in glass. Figure 3 compares the Sb(III) content in  $\text{Sb}_2\text{O}_5$  oxide with the same oxide doped into glass by thermal treatment at a temperature from  $650$  to  $800^\circ\text{C}$ . About a half of the antimony is converted from Sb(V) to Sb(III) for pure oxide in this range of temperature, while the

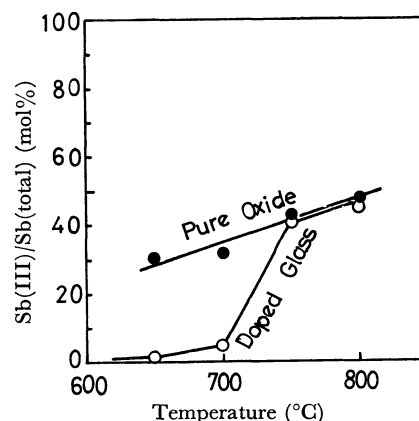


Fig. 3. Variation of Sb(III) content by thermal decomposition in the  $\text{Sb}_2\text{O}_5$  as pure oxide and the  $\text{Sb}_2\text{O}_5$  doped in  $\text{NaPO}_3$  glass in a temperature range  $650$  to  $800^\circ\text{C}$ .

19) E. R. Johnson; "Radiation Induced Decomposition of Inorganic Molecular Ions", Gordon & Breach, N. Y. (1970), p. 23.

20) D. I. Stewart, *Can. J. Chem.*, **50**, 690 (1972).

antimony in the glass remains practically unchanged in the oxidation state below the temperature of 700 °C probably because of a slow diffusion in the viscous medium of the molten glass. The results in Fig. 3 demonstrate that the conversion from Sb(V) to Sb(III) tends to a composition corresponding to  $\text{Sb}_2\text{O}_4$  or  $\text{Sb}_6\text{O}_{13}$  at the temperatures used in this work. The oxidation of Sb(III) to Sb(V) in glass, when  $\text{Sb}_2\text{O}_3$  is doped, is not significantly induced by atmospheric oxygen during the preparation of glass in the temperature range from 600 to 900 °C. The radiation-induced reaction of redox between Sb(III) and Sb(V), which occurs in the directions of both oxidation and reduction, may be related to the stabilization of the oxidation state approximately equal to +4 not only in molten glass but also in quenched, Sb-doped glass. The  $\text{Sb}_2\text{O}_4$  or  $\text{Sb}_6\text{O}_{13}$  is, therefore, in transient equilibrium with dissociated oxygen or oxygen in the atmosphere at high temperatures and results in the formation of defects or the excess of oxygen in quenched Sb-doped glass. The abnormally high *G*-values of the redox of antimony may be closely connected with the effect of oxygen<sup>21)</sup> involved in the radiation induced redox of antimony oxides in polyphosphate glass.

**Optical Absorption of Antimony-Doped Glass.** Figure 4 illustrates the change in the optical absorption for antimony-doped polyphosphate glass under the influence of  $\gamma$ -radiation with a dose up to  $3 \times 10^{18}$  eV/g. Curves I and II are for the glasses doped with 1 mol% of  $\text{Sb}_2\text{O}_3$  and  $\text{Sb}_2\text{O}_5$  respectively; curves III and IV are for  $\gamma$ -irradiated samples of these two glasses. Non-irradiated samples absorb in near-ultraviolet region and appear colorless, while the  $\gamma$ -irradiated samples are colored pale yellow for  $\text{Sb}_2\text{O}_3$ -doped glass irradiated with a high dose of  $5 \times 10^{20}$  eV/g. This increased absorption caused by radiations implies that the conversions of Sb(III) to Sb(V) and in the reverse direction occur in an appreciable degree to produce an interaction absorption such as is frequently encountered

in mixtures of Sb(III) and Sb(V) compounds.<sup>22)</sup> Interaction absorption is observed for chloride mixtures of Sb(III) and Sb(V) as well in an aqueous solution as in a solid, but not for the oxide mixtures. In a highly-polarizable halide system these mixtures have an intense optical absorption in the visible region and are colored black in a solid and they are diamagnetic. According to our ESR study, there was no observable signal which could be assigned to tetravalent antimony radicals in the  $\gamma$ -irradiated Sb-doped glass. It is quite possible to assume that the radiation-induced Sb species of an intermediate state between Sb(III) and Sb(V) is a cause of the strong interaction in the optical-absorption property.

**Mo-doped Glass, Effects of Molybdenum Ions.** For investigating the effect of molybdenum ions on the radiation-induced holes and electrons in polyphosphate glass, three glasses with different contents of Mo(VI) and Mo(V) were employed. They were prepared by introducing 0.5 to 1 mol% of  $\text{MoO}_3$  into sodium dihydrogen phosphate for dehydration in the presence or absence of adequate reducing agents, such as ammonium oxalate; they were then melted by controlling the atmosphere with carbon rods piled around a graphite crucible so as to exclude the air as much as possible in the electric furnace. The oxidation states of the molybdenum ions in these samples were determined by a potentiometric titration of Mo(V) with  $\text{K}_2\text{Cr}_2\text{O}_7$ .<sup>14)</sup> The results are 100% of Mo(VI) for Mo(VI)-rich glass, 35 to 40% of Mo(V) in the glass with a medium Mo(V) content, and 95% of Mo(V) at a maximum in the Mo(V)-rich glass. The Mo(VI)-enriched glass with a total Mo-content of 0.5 to 1.0 atom % has no optical absorption in the visible and near-ultraviolet regions, and the diamagnetic Mo(VI) ions in this glass show no ESR signal. On the other hand, the Mo(V)-enriched glass has a deep bluish-green color and an absorption maximum at 810 nm;

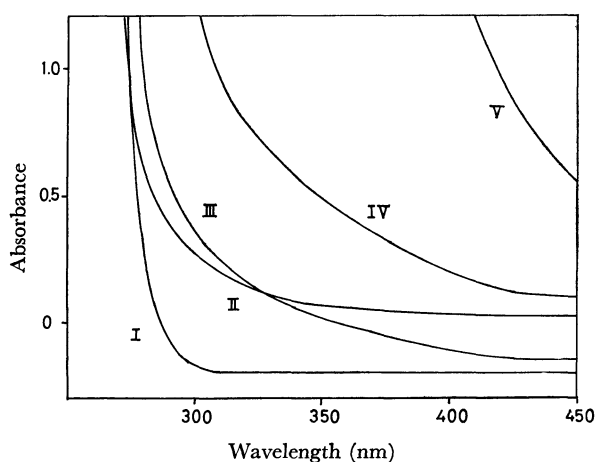


Fig. 4. Optical absorptions of  $\gamma$ -irradiated polyphosphate glass containing one mol % of antimony oxides. Curves I and II: Non-irradiated and  $\gamma$ -irradiated  $\text{NaPO}_3$  glass with 1 mol %  $\text{Sb}_2\text{O}_3$  doped, respectively. Curves III and IV: The same as above (I and II) with 1 mol %  $\text{Sb}_2\text{O}_5$  doped.

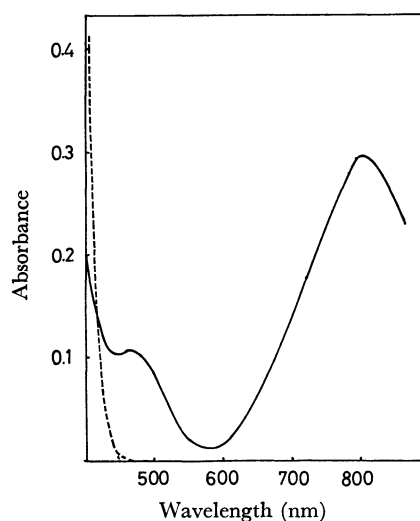


Fig. 5. Absorption spectra of polyphosphate glass containing molybdenum (V) and molybdenum (VI) (indicated by broken line).

21) J. G. Rabe, *Ber.*, **71**, 108 (1967).

22) J. Whitney and N. Davison, *J. Amer. Chem. Soc.*, **76**, 3809 (1949).

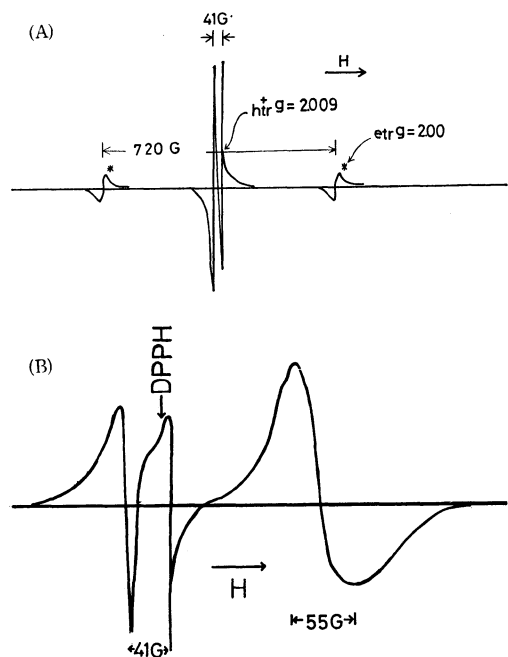
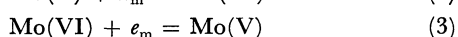
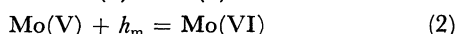


Fig. 6. ESR spectra of  $\gamma$ -irradiated polyphosphate glass. (A) non-doped glass with holes  $h_{tr}$  and electrons  $e_{tr}^*$  (identified as  $PO_3^{2-}$ )<sup>7)</sup> (B)  $Mo(VI)O_3$  doped glass with holes  $h_{tr}$  (right hand doublet) and  $Mo(V)$  signal ( $g=1.917$ )

the molecular extinction coefficient was determined, by using a sample 8 mm thick between two opposed flat surfaces, to be  $\epsilon=17 \text{ M}^{-1} \text{ cm}^{-1}$ . The latter spectrum is illustrated in Fig. 5. Figure 6 shows the ESR spectrum of the  $Mo(V)$ -containing glass; there is a broad singlet of  $g=1.917$ , with 55 Gauss peak-to-peak width which is attributable to the  $Mo(V)$  in the glass.<sup>23-25)</sup>

Under  $\gamma$ -irradiation, the  $Mo(VI)$ -rich glass is red in color and the optical absorption at 510 nm increases with an increase in the absorbed  $\gamma$ -doses. On the contrary,  $Mo(V)$ -rich glass, colored bluish-green before irradiation, loses its original color by absorbing radiation energy, but shows no intensity change in the optical absorption at 510 nm due to trapped holes. In  $Mo(VI)$ -rich glass, ESR signals of the hole doublet and the  $Mo(V)$  singlet appear after irradiation, as is shown in Fig. 6; these two signal intensities grow as the absorbed radiation dose increases. The singlet due to  $Mo(V)$  continues to increase after the hole doublet attains saturation. In  $Mo(V)$ -enriched glass, no hole signal could be detected up to a sufficiently large  $\gamma$ -dose of  $1.5 \times 10^{22} \text{ eV/g}$ . Accordingly, dopant molybdenum in the polyphosphate glass is effective for trapping both holes and electrons produced by  $\gamma$ -radiations through Processes (2) and (3):



In Eqs. (2) and (3),  $h_m$  and  $e_m$  are the mobile holes and electrons. Besides the processes postulated by (2) and

(3), there must be several other reactions, involving trapping by the glass matrix and the recombination of holes and electrons through a certain recombination center. However, there is no means of detecting the recombination yields or of distinguishing the trapped holes and electrons in the glass matrix from those obtained in the presence of molybdenum.

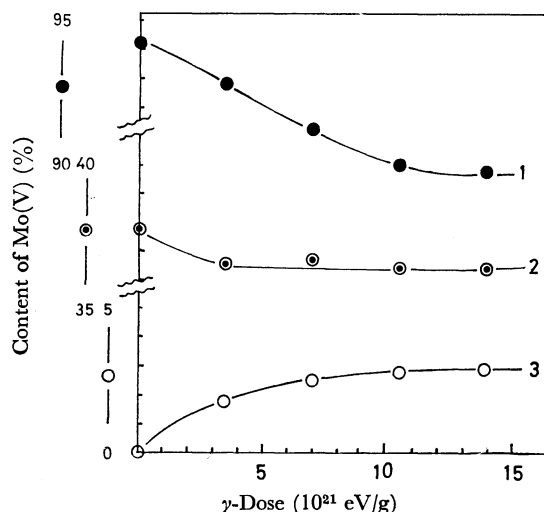


Fig. 7. Variation of  $Mo(V)$  content by radiation-effect in polyphosphate glass with total Mo 1 atom % per phosphorus.  $\bullet$ :  $Mo(V)$  rich glass (94%  $Mo^V$ ),  $\odot$ : glass with medium content of  $Mo(V)$  (37%  $Mo^V$ ),  $\circ$ :  $Mo(VI)$  rich glass ( $Mo^V$  trace)

**Quantitative Estimation of the Dose Effect.** The  $Mo(V)$  formation through Reaction (3) and the loss of  $Mo(V)$  through (2) in the irradiated glass were determined by studying the intensity changes in the optical absorption; the results are shown in Fig. 7. Curve 1 is for  $Mo(V)$ -rich glass; its optical density decreases in proportion to the absorbed  $\gamma$ -doses up to the dose of about  $1.0 \times 10^{22} \text{ eV/g}$ . Beyond this limit, no further decrease of  $Mo(V)$  was observed. At the maximum dose of  $1.5 \times 10^{22} \text{ eV/g}$ , four percent of doped  $Mo(V)$  was converted into  $Mo(VI)$ ; the  $G$  value calculated from the linear part of the curve is 0.11. Curve 3 is  $Mo(VI)$ -rich glass containing no detectable  $Mo(V)$ , but exhibiting the green color of  $Mo(V)$  after irradiation. The radiation-induced formation of  $Mo(V)$  from  $Mo(VI)$  is less than 0.03 mol% even at  $1.5 \times 10^{22} \text{ eV/g}$ . Curve 2 is the intermediate case for the irradiated glass which contains comparative amounts of  $Mo(V)$  and  $Mo(VI)$ . The curve shows little optical absorption change except for that in the very small dose region. Consequently, there must be a stationary condition of redox reaction between  $Mo(V)$  and  $Mo(VI)$  at a  $Mo(V)/Mo(VI)$  ratio in the proximity of 1 to 2, if one mol % of Mo is present in the glass.

The trapping of holes and the conversion of  $Mo(VI)$  to  $Mo(V)$  through Reaction (3) are parallel reactions; the rates of the two processes can be followed by measuring the relative intensities of ESR signals for the hole doublet and the  $Mo(V)$  singlet. Figure 6B shows the use of these two ESR signals for estimating the relative concentration of trapped holes and  $Mo(V)$  in  $\gamma$ -irradiated glass. The observed ratio of trapped

23) K. S. Sechacli and L. Petrakis, *J. Phys. Chem.*, **74**, 4102 (1970).

24) P. R. Edwards and S. Subramanian, and M. C. R. Symons, *Chem. Commun.*, **1968**, 799.

25) R. D. Dowsing and J. F. Gibson, *J. Chem. Soc., A*, **1967**, 655.

TABLE 1. TRAPPED HOLES TO Mo(V) CONCENTRATION RATIO,  $[h^+]/[Mo(V)]$ , MEASURED BY ESR ABSORPTION INTENSITIES IN  $\gamma$ -IRRADIATED Mo (1 ATOM %) DOPED GLASS

Mo(V) concentration [Mo(V)]/[Mo(total)] %	$\gamma$ -Dose (10 eV/g)			
	3.6	7.2	10.8	14.5
Mo(V) enriched (94%)	0	0	0	0
Medium Mo(V) (35–40%)	0.64	1.27	1.11	1.45
Mo(V) poor (Mo(V) absent)	19.3	19.1	19.2	19.3

holes to produced Mo(V),  $[h^+]/[Mo(V)]$ , is represented in Table 1. For Mo(VI)-rich glass, this ratio is 19.3, independent of the absorbed dose, while the glass containing comparative amounts of Mo(V) and Mo(VI), but slightly higher in Mo(VI), shows a  $[h^+]/[Mo(V)]$  ratio 30 times lower. There is no trapped hole formation in Mo-doped glass if most of the Mo is present in the Mo(V) state. On the basis of these observations it is clear that the trapping of either holes or electrons, and also the transmutation of states from Mo(VI) to Mo(V) and in the reverse direction through Paths (3) and (2) respectively, depend on the Mo(VI)/Mo(V) ratio and on the total content of Mo in the irradiated glass.

**Thermal Annealing.** By the application of the usual temperature-elevating device of ESR attachment, an attempt was made to study the stability of holes and Mo(V) radicals.<sup>26)</sup> There are two ESR signals attributable to the trapped holes and the Mo(V). Upon heating at 200 °C for 15 min the doublet signal due to holes disappears at once. By this thermal treatment the radiation-induced red color of the glass is lost, leaving a faint yellow color behind. Isothermal annealing were made at two fixed temperatures, 110 and 147 °C, by recording the changes in the peak height of the ESR signals every minute. As these isothermal curves are exponential, logarithmic plots of the signal intensity are illustrated in Fig. 8; these plots demonstrate the rapid decay of hole signals along with the invariant intensities of the Mo(V) singlet. Annealing at two temperatures allows us to estimate roughly the activation energy of hole decay. If thermal annealing can be explained only in terms of a recombination of holes with electrons, the decay of trapped holes obeys a bimolecular mechanism, but there is no experimental evidence to prove emission due to recombination during thermal treatment. By means of unimolecular mechanism the activation energy which reflects the average energy required for the escaping of trapped holes from a certain trap depth present in the irradiated polyphosphate matrix can be estimated. From the curves in Fig. 8, the value is found to be 0.37 eV. As for the high stability of the Mo(V) produced by irradiation, it can be understood by taking account of the special stability of molybdenum blue oxide,  $Mo_nO_{3n-1}$ , as a polymer form which might be present in polyphosphate glass.

26) C. Bettinali and P. Granati, *Z. Phys. Chem. N. F.*, **70**, 24 (1970).

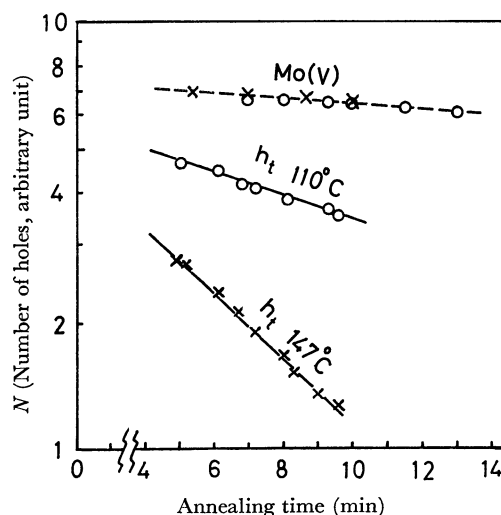


Fig. 8. Isothermal annealing curves of irradiated glass containing Mo(V) by logarithmic plots of the intensity of ESR signal at 110 °C and 147 °C

**U-Doped Glass, Effect of Uranium.** The absorption spectrum of  $U_3O_8$ -doped glass before  $\gamma$ -irradiation is shown in Fig. 9. By the chemical analysis of this glass, containing 1.0 atom percent of uranium per phosphorus, the content of U(IV) was found to be 32.4% of the total uranium, while the rest of uranium was U(VI). The  $UO_3$ -doped glass prepared by dehydrating a mixture of  $NaH_2PO_4$  and  $UO_2(CH_3CO_2)_2$  and by subsequent melting in open air is yellow in color and has no detectable U(IV). The broken curve in Fig. 9 shows a visible absorption due to U(VI) alone observed in the  $UO_3$ -doped glass, with a maximum located at 423 nm. By heating uranylacetate in a vacuum at from 800 to 900 °C for a hundred hours, a grey-black oxide was obtained; its U(IV) content was as large as 59% and it had the approximate composition of  $UO_{2.4}$ . The glass doped with 1 mol% of this oxide is green and has several visible absorption peaks, at 1120, 662, 545, 483, and 423 nm. The last one, 423 nm, may be ascribed to U(VI) and remains little affected by the variation in the U(IV) content in the glass. Table 2 compares the optical absorption at these peaks and the contents of U(IV) measured by chemical analysis<sup>16)</sup> in three types of glass samples, with  $UO_3$ ,  $U_3O_8$ , and  $UO_{2+x}$  as dopants. The molecular extinction was  $32.1 \text{ M}^{-1} \text{ cm}^{-1}$  for U(IV), as determined by the maximum peak at 1120 nm.

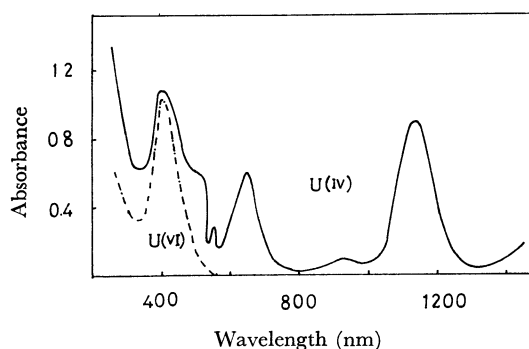


Fig. 9. Optical absorption spectra of U(IV) (full line) and U(VI) (broken line) in polyphosphate glass.

TABLE 2. OPTICAL ABSORPTION AT MAXIMUM PEAKS FOR URANIUM DOPED GLASSES (TOTAL URANIUM CONTENT 1 ATOM % TO P in  $\text{NaPO}_3$  GLASS)

[U(IV)]/[U(total)] %	Doped oxide		
	$\text{UO}_{2+x}$ 55%	$\text{U}_3\text{O}_8$ 27%	$\text{UO}_3$ 0.0
Wavelength $\lambda(\text{nm})$	423	0.18 (0.13) <sup>a)</sup>	0.21 (0.18) <sup>a)</sup>
	483	0.1	0.05
	545	0.1	0.05
	662	0.26	0.13
	1120	0.38	0.19

a) The values in parentheses show the optical densities calculated from U(VI) based on the value of 0.26

**The Effect of  $\gamma$ -Radiation on Uranium.** Exposure of  $\text{U}_3\text{O}_8$ -doped glass to  $\gamma$ -radiation produced a ESR singlet, with  $g=2.6$  and a peak-to-peak width of 762 G, which was bleached by natural aging for one week. This type of ESR signal is shown in Fig. 10, along with the signals due to the holes and electrons trapped as usual found in the glass matrix. A similar type of ESR spectrum reported by Selbin<sup>27)</sup> *et al.*, in thorium oxide and other halide compounds closely resembles ours in line shape and peak-to-peak width, but is very different in  $g$ -value ( $g=1.52$ ). In  $\text{UO}_{2.4}$ -doped glass as well as in  $\text{UO}_3$ -doped polyphosphate glass, there were no other signals than holes and electrons trapped in the glass matrix when the glass was irradiated with  $\gamma$ -rays. Although no direct support of the formation of U(V) in the irradiated glass is available as a result of chemical analysis or optical-absorption measurements,<sup>28)</sup> this center might be intimately related to the  $[\text{U}(\text{IV})+h_m^+]$  center. Consequently, a metastable oxidation state of U(V) exists at room temperature only as a transient state from U(IV) to U(VI).

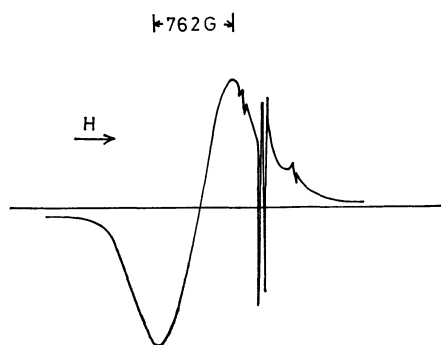


Fig. 10. ESR spectrum of  $\gamma$ -irradiated polyphosphate glass containing uranium(IV) ions, broad line at left with  $g=2.6$  assigned to U(V).

**Radiation-induced Redox Yields.** Conversion between U(IV) and U(VI) and a reaction in the reverse direction in glass under the effect of  $\gamma$ -radiation are shown in Fig. 11. The optical absorption changed at 1120 nm, and the chemical analysis of U(IV)<sup>16,28)</sup> was followed by irradiation as a function of the  $\gamma$ -dose. Curve a is

27) J. Selbin and J. D. Ortego, *Chem. Rev.*, **69**, 6570m (1969).

28) D. A. Wenz, M. D. Adams, and R. K. Steuhenberg, *Inorg. Chem.*, **3**, 989 (1964).

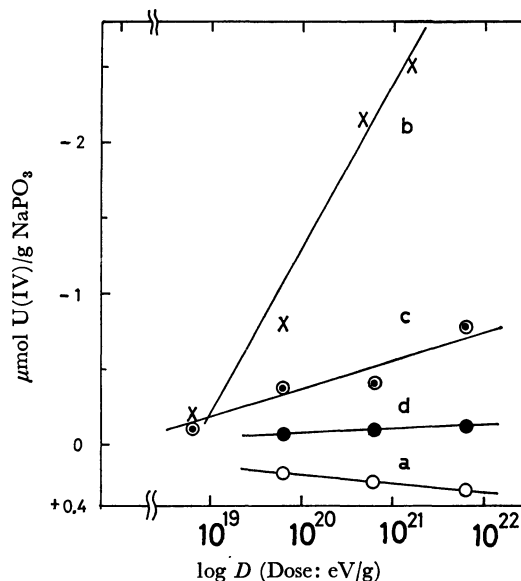


Fig. 11. Variation of U(IV) content as function of absorbed  $\gamma$ -energy in polyphosphate glass a: glass containing  $\text{U}^{\text{VI}}$  1.00%, b: glass with  $\text{U}^{\text{IV}}$  0.093%, c: glass with  $\text{U}^{\text{IV}}$  0.32% and  $\text{U}^{\text{VI}}$  0.201%, and d: glass with  $\text{U}^{\text{IV}}$  0.32% and  $\text{U}^{\text{VI}}$  0.64%.

for 1 mol%  $\text{UO}_3$  doped glass; it shows that the increase of U(IV) produced by irradiation is so slight as to be measured only by a logarithmic increase in the  $\gamma$ -dose. Curve d is for  $\text{U}_3\text{O}_8$ -doped glass with 0.32 atom % of U(IV) and 0.64 atom % of U(VI); it shows a continuous decrease in U(IV) with an increase in the  $\gamma$ -dose, but at a slower rate than in the case of curve c. At small doses, trapped holes are hard to detect by optical absorption, while ESR doublet signals due to holes begin to appear at a dose of  $6 \times 10^{18}$  eV/g. Curve c is for a glass sample containing 0.60 atom % of U(IV) and 0.20 atom % of U(VI), with an approximate dopant composition of  $\text{UO}_{2.25}$ . This sample glass shows an appreciable decrease in U(IV) content when it is exposed up to  $6.4 \times 10^{21}$  eV/g. These results Curves a, d and c, demonstrate that the exposure of uranium doped glass to  $\gamma$ -radiation causes the conversion of U(IV) to U(VI) or a reverse process, depending on the  $\text{U}(\text{IV})/\{\text{U}(\text{IV})+\text{U}(\text{VI})\}$  ratio in the glass before irradiation. The yields of the conversion in the oxidation state of uranium have a minimum in the glass

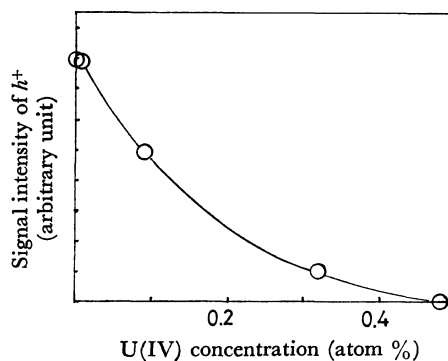


Fig. 12. ESR signal intensity of U(V) produced by  $\gamma$ -irradiation as metastable  $(\text{U}(\text{IV})+h_m^+)$  center as function of U(IV) concentration in polyphosphate.

with a  $U(IV)/\{U(IV)+U(VI)\}$  ratio at approximately 1:2, corresponding to the  $U_3O_8$  composition.

As for the trapped holes thus produced, the intensities of the ESR doublet signals are greatly reduced by an increase in the doped  $U(IV)$  content, according to the exponential law shown in Fig. 12. Stroud's equation (1) provides an effective capture volume of  $U(IV)$  ions for dry or mobile holes that can be estimated to be  $2.58 \times 10^4 \text{ \AA}^3$  from the curve in Fig. 12; this indicates a much smaller value than  $3.8 \times 10^5 \text{ \AA}^3$  in the case of  $Sb_2O_3$  as the dopant. The results in Fig. 12 also demonstrate that 40% of the dopant uranium must be present in the +4 oxidation state for the complete suppression of the trapped holes when 1.0 atom % uranium-doped glass is exposed to  $\gamma$ -radiation with a dose of  $6 \times 10^{19} \text{ eV/g}$ . The maximum  $G$  values for the oxidation of  $U(IV)$  to  $U(VI)$  were obtained by doping 0.1 atom % of  $UO_2$  oxide in a vacuum; they showed that 93% of uranium present in the +4 oxidation state. They are calculated to be 1.3 at  $6 \times 10^{19} \text{ eV/g}$  and 0.833 at  $6 \times 10^{20} \text{ eV/g}$  from the data shown by Curve b in Fig. 11.

### Conclusion

For the three systems of redox couples that we have investigated, each has a minimum yields of radiation-induced redox at the concentration corresponding to these compositions;  $Sb_2O_4$  for the  $Sb(III)$ – $Sb(V)$  system,  $Mo_6O_{17}$   $\{Mo(V):Mo(VI)=1:2\}$  for the  $Mo(V)$ – $Mo(VI)$  system, and  $U_3O_8$  for the  $U(IV)$  and  $U(VI)$  system, in polyphosphate glasses.

The effective capture volumes are  $3.8 \times 10^5 \text{ \AA}^3$  for  $U(IV)$  ions, with respect to the trapping holes.  $Mo(V)$  ions take an intermediate value between  $Sb(III)$  and

$U(IV)$  ions.

Abnormally high radiation yields are observed when antimony oxide is used as the dopant; this is, probably, a particular case of an antimony oxide system whose gas-cleaning action has been used in the glass industry, because of its high oxygen pressure of thermal decomposition.

The approximate  $G$  values are 0.9 for 0.57 mol% of  $Sb_2O_3$  and 0.43 mol% of  $Sb_2O_5$ , 0.7 for 0.31 mol% of  $Sb_2O_3$  and 0.69 mol% of  $Sb_2O_5$ , with respect to the formation of  $Sb_2O_3$  at  $1 \times 10^{21} \text{ eV/g}$ . The  $G$  values of the formation of  $Mo(V)$  from  $Mo(VI)$  are 0.54 for 0.5 atom % of  $Mo(VI)$ -doped glass and 0.18 for 1.0 atom % of  $U(IV)$  and a trace of  $U(VI)$ . They are 1.3 at  $6 \times 10^{19} \text{ eV/g}$  and 0.833 at  $6 \times 10^{20} \text{ eV/g}$ . A more sensitive method of analysis of the product is required for a further discussion in detail of the  $G$  values, particularly of the initial  $G$  values, which are computed in a very-small-dose region.

A kinetic study of the rate of annealing indicates an unimolecular mechanism, providing an activation energy of 0.37 eV for bleaching trapped holes. In the case of  $Mo$ , the redox processes between the two oxidation states involve only one electron. In the cases of  $Sb$  and  $U$ , the difference in oxidation number is two. In these two cases, no conclusive identification of  $Sb(IV)$  and  $U(V)$  was obtained. However, strong evidence for the formation of an intermediate oxidation state has been presented, and it can be assumed that the redox reactions involved proceed through an one-electron step.

The authors wish to express their thanks to Dr. A. Barkatt, the University of Israel, for his valuable advice.